scientific data

OPEN

DATA DESCRIPTOR

High-resolution gridded dataset of China's offshore wind potential and costs under technical change

Kangxin An[1], Wenjia Cai[2], Xi Lu[1,3] & Can Wang[1,3] ✉

Assessing the dynamics of offshore wind potential and costs is essential for low-carbon energy policy decision-making and energy modeling, but no open-source, spatial explicit and technologically detailed dataset is available. This study addresses this gap by employing a consistent assessment framework that integrates GIS analysis, a wind reanalysis model, a component-based cost model and scenario analysis. It identifies suitable space for offshore wind deployment considering 12 technical and policy constraints, estimates hourly output curves, capacity factors, and technology cost dynamics by components across 5058 grid points with a 10 km resolution from 2020 to 2035 under three technical change scenarios. The dataset has been validated through comparisons with existing offshore wind projects and datasets, and is stored in two formats (GeoTIFF and NetCDF4). This dataset offers extensive potential for use as an input in climate policy and energy system research.

Background & Summary

The transition to a net-zero emissions energy system is essential for meeting both global and national climate goals, necessitating the large-scale and rapid development of renewable energy to replace fossil fuels[1–3]. The rapid decline in the costs of wind, solar, and energy storage technologies is accelerating the decarbonization of power systems[4–6]. However, a range of factors, such as spatial mismatches between electricity supply and demand[7], transmission infrastructure planning[8], land use policies[9], and business models for distributed renewables[10], are driving offshore wind to play a crucial role in meeting the growing electricity demands of coastal regions in China[11]. By 2023, China's cumulative installed capacity for offshore wind power has exceeded 37 GW, with projections suggesting it could reach 141 GW by 2030[12]. Nonetheless, the potential and costs of offshore wind exhibit significant spatial heterogeneity, and uncertainties regarding technical change could substantially affect the scale of offshore wind deployment. Considering existing datasets on energy resources or technologies provide valuable insights[13–15], creating a consistent, high-resolution, open-source dataset of offshore wind potential and costs in China, accounting for uncertainties in technical change, is crucial for energy planning and climate studies. Currently, no such dataset is available.

Offshore wind potential and costs under technical change have been widely studied from four key aspects. First, existing research highlights significant regional and seasonal variations in offshore wind energy resources[16], with the northern South China Sea exhibiting the highest wind energy density[17]. Therefore, high-resolution assessments of offshore wind capacity factors and hourly output curves have been conducted across various regions to capture the spatiotemporal variability of wind energy generation potential, based on wind reanalysis data[9,18–20]. Second, regulatory requirements limit the capacity potential of offshore wind, including maritime rights, water depth, offshore distance, protected areas, and competing marine uses[21–23]. Constraints from shipping lanes, cables and pipelines, bird migration paths and visibility are estimated to reduce the available technical potential by 8.7%[22]. Third, spatial factors such as offshore distance and water depth influence the selection and costs of foundation types and transmission technologies[24]. Existing literatures have assessed lifecycle costs of offshore wind farm cases[25–28] or mapped the spatial distribution of costs[24,29–31] in European countries to capture the spatial heterogeneity of technology costs. Some studies have also evaluated high-resolution offshore wind costs in China[11,21,22,32]. Fourth, technical change impacts offshore wind costs through multiple

[1]State Key Joint Laboratory of Environment Simulation and Pollution Control (SKLESPC), School of Environment, Tsinghua University, Beijing, 100084, China. [2]Ministry of Education Key Laboratory for Earth System Modeling, Department of Earth System Science, Tsinghua University, Beijing, 100084, China. [3]Institute for Carbon Neutrality, Tsinghua University, Beijing, 100084, China. ✉e-mail: canwang@tsinghua.edu.cn

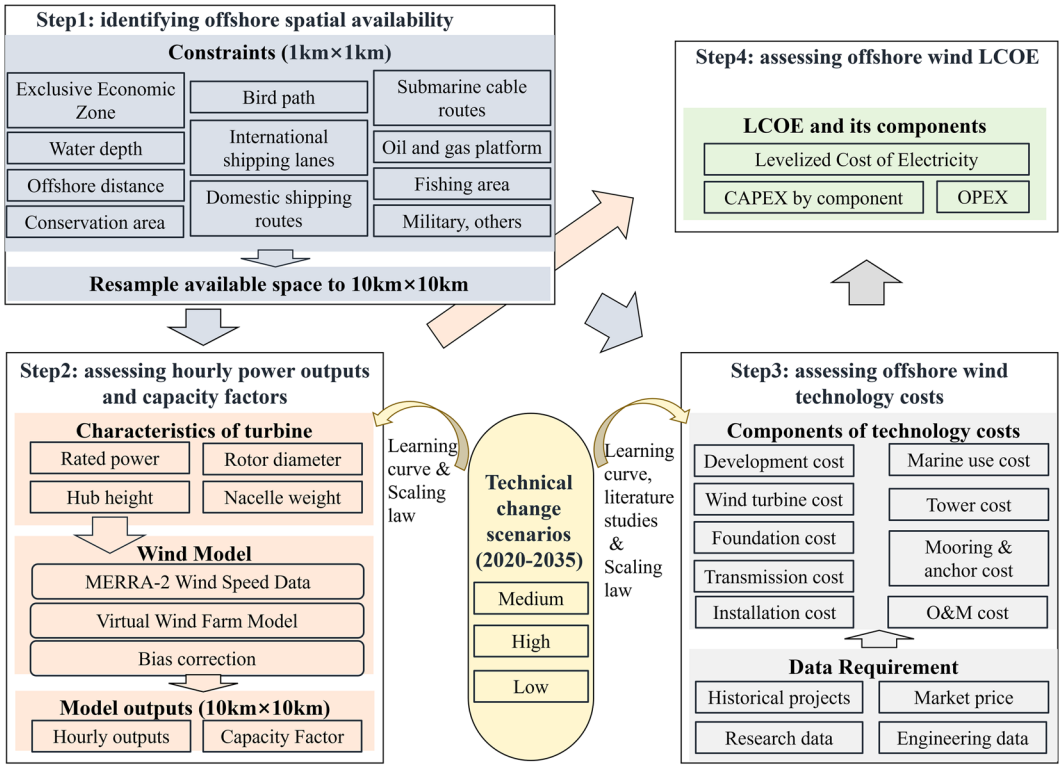

Fig. 1 Overview of offshore wind potential and cost assessment procedures.

channels. The Levelized Cost of Energy (LCOE) for offshore wind is projected to decrease by 40–49% by 2050 compared to 2019, driven by improvements in capacity factors, design life, and reductions in investment, operation and capital costs[33]. The cost of floating offshore wind is expected to reduce faster than fixed-bottom offshore wind, leading to the spatial heterogeneity of the impacts of technical change, depending on site characteristics and technological choices made across different spatial grids[34].

However, three key research gaps need to be addressed. First, existing studies fail to incorporate the restrictions on offshore wind availability, or have not fully consider actual policy constraints when estimating offshore wind potential. Second, studies on China ignored technological details or fail to utilize sufficient engineering data to estimate the offshore wind cost by components in detail. A high-resolution component-based cost model is needed to enhance transparency in analyzing the spatial heterogeneity of offshore wind cost dynamics. Third, few studies have analyzed the channels, uncertainties, and spatial variability of impacts of offshore wind technical change, which is important for energy planning and modeling. Therefore, we propose a spatially explicit and internally consistent assessment framework for offshore wind resources and costs in China, by integrating GIS, a wind reanalysis model, a component-based cost model, and scenario analysis. We identify offshore spatial availability considering 12 technical and policy constraints, simulating hourly wind power output, capacity factor, and technology cost dynamics by components of 5058 grid points at 10 km resolution from 2020 to 2035 under three technical change scenarios. The framework ensures accurate and consistent assessment on potential and costs under technical change, and the dataset is stored in two formats (GeoTIFF and NetCDF).

Methods

The assessment framework consists of four modules (Fig. 1). First, we identify gridded offshore spatial availability by extracting 12 types of constraint conditions based on GIS, ensuring no conflicts with other marine use activities. Second, we assess gridded offshore wind hourly output curves and capacity factors under three technical change scenarios, using NASA's MERRA-2 wind speed reanalysis data[35] and a virtual wind farm model[20]. Third, we develop a gridded offshore wind cost assessment model with nine components of developing, manufacturing, installation and O&M costs. The model assesses the technological selection and costs based on offshore distance and water depth of each grid, and analyzes cost reduction dynamics using learning curves and expert judgments. Fourth, we analyze the LCOE and its components for offshore wind for each grid.

Step1: Identification of offshore space availability. Table 1 summarizes 12 constraints derived from actual policies and existing research[21–23], including EEZ, water depth, two offshore distance criteria, two natural reserve conditions (i.e., coastal conservation areas and bird migration paths), and six types of competing marine uses (i.e., international shipping lanes, domestic shipping routes, submarine cable routes, oil and gas platforms, fishing areas, military zones and other restricted areas). Using GIS tools, we eliminated all restricted areas, retaining only the available offshore space at a 1 km resolution. Given that offshore wind farms may cause visual and

Constraint	Description	Data Source
Maritime rights	Limited to the Exclusive Economic Zone along the China mainland coastline	Flanders Marine Institute, EEZ v12[47]
Water depth	Not exceeding 1000 m	ETOPO 2022[48]
Offshore distance	Offshore distance greater than 10 km and water depth exceeding 10 m	Chinese government, 2011
	Offshore distance greater than 30 km or water depth exceeding 30 m	Chinese government, 2023
Natural reserve	Prohibit construction in China's coastal conservation areas and within a 1 km buffer zone.	Bohorquez *et al.*[49]
	Prohibit construction in bird migration paths and within a 5 km buffer zone	Yong *et al.*[50]
Competing marine use	Prohibit construction in international major shipping lanes and within a 3 km buffer zone.	Benden[51]
	Prohibit construction in domestic coastal shipping routes and within a 3 km buffer zone.	China Geographic Atlas[52]
	Prohibit construction along submarine cable routes and within a 0.5 km buffer zone.	TeleGraphy[53]
	Prohibit construction near oil and gas drilling platforms and within a 0.5 km buffer zone.	Global Energy Monitor[54]
	Prohibit construction in coastal fishing zones.	Halpern *et al.*[55]
	Prohibit construction in military and other restricted areas.	China Nautical Chart[56]

Table 1. Constraints on China's offshore wind deployment.

noise pollution, and competition for marine space, the Chinese government mandates that offshore wind farms be located at least 10 km from shore and in waters deeper than 10 m, with additional requirements for distances beyond 30 km or depths exceeding 30 m, as specified in regulations from 2011 and 2023, respectively. After identifying the available space, we adjusted its resolution to 10 km using a resampling method, which preserves spatial information and reduce data redundancy.

Step2: Gridded assessment of hourly outputs and capacity factors. We set three technical change scenarios, i.e., medium, low and high, to evaluate dynamics of hourly output curves and capacity factors of offshore wind. We first consider 4 key characteristics of offshore wind turbines: rated power, rotor diameter, hub height, and nacelle weight. Rated power has increased rapidly since 2018. Assuming a one-year lag between the bidding and construction periods, we simulate the growth dynamics of rated power based on a one-factor learning curve, using historical cumulative installed capacity and rated power data from 2018 to 2023. The learning rate is estimated at 29%, with a 90% confidence interval ranging from 18% to 40%. Based on installed capacity projections[12], the average rated power is projected to reach 19.1 MW (with a range of 15.2 to 24.1 MW) by 2035. Using the scaling laws of wind turbines[36], the relationships between rated power (P), hub height (H), and nacelle weight (W) are modeled as power functions of rotor diameter (D), as shown in Eq. (1), where "Var" represents P, H and W. The power function parameters, along with the predicted values for individual turbine capacity in 2025, 2030, and 2035, are represented in Table 2. The average hub height is projected to reach 163, 148, and 179 m under medium, low and high scenarios, respectively.

$$Var = aD^b \tag{1}$$

To assess the hourly output curves and capacity factors of offshore wind, and the impact of hub height changes under three scenarios, we employ the Virtual Wind Farm (VWF) model[20], and use NASA's MERRA-2 reanalysis hourly wind speed data in 2020[35]. The model obtains wind speed data at heights of 2, 10, and 50 m, then interpolates the wind speeds to each grid using LOESS regression. It extrapolates the wind speed to hub heights using the logarithmic profile law, and ultimately converts the wind speed to power output using smoothed turbine power curves. Due to biases in the wind speed reanalysis data, the modeled capacity factors often exceed the observed ones. The VWF model defines the systematic error ε_{CF} as the ratio of observed capacity factors to simulated capacity factors for a given country or region. The error is used to correct the wind speed data through a linear adjustment, as shown in Eq. (2), allowing for the correction of predicted capacity factors at each grid point.

$$\omega' = \alpha\omega + \beta,\ s.\ t.\ \overline{P(\omega')} = \varepsilon_{CF}\overline{P(\omega)} \tag{2}$$

where ω denotes the reanalysis wind speed data, ω' denotes the corrected wind speed data, and α and β are the correction parameters. $\overline{P(\omega')}$ and $\overline{P(\omega)}$ represent the average capacity factors simulated using the corrected wind speed data and the original reanalysis data, respectively. α is assumed to be a function of ε_{CF}, such that $\alpha = 0.6\varepsilon_{CF} + 0.2$, while β needs be fitted.

We estimate ε_{CF} by applying the VWF model, using hourly wind speed data for the year 2020 from the MERRA-2 dataset, and the parameters for the Vestas 8.0 MW turbine[9]. The locations of offshore wind farms installed before 2020 are sourced from a global offshore wind turbine dataset[37]. Considering an average rated power of 4.8 MW in 2020, the corresponding hub height is set to 92 m based on Eq. (1). The average capacity factor is 33.1%, which is higher than the actual value of 28.5%. Thus, ε_{CF} is estimated as 0.86, which is close to the simulated value of 0.82 for the UK[20]. Based on this, α is set to 0.72, while β is determined to be 1.81 m/s through iterative searching using the VWF model. With these corrections, we then evaluate the hourly output curves and capacity factors for offshore wind power at each grid under three scenarios.

Characteristics	Unit	a	b	2025	2030	2035
Rated power (P)	W	8.207e-4	1.79	11.9(11.1–12.8)	15.8(13.4–18.7)	19.1(15.2–24.1)
Rotor diameter (D)	m	1	1	211(203–220)	248(226–272)	275(242–313)
Hub height (H)	m	2.41	0.75	134(130–137)	151(140–161)	163(148–179)
Nacelle weight (W)	t/MW	24.3	1.88	47.9(47.8–48.1)	48.6(48.2–49.0)	49.1(48.5–49.7)

Table 2. Function parameters and predicted values of wind power turbine.

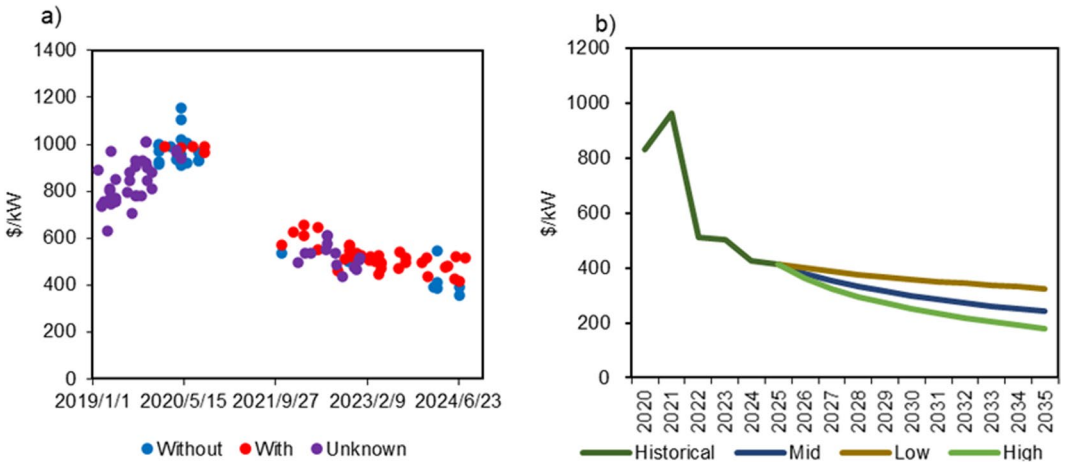

Fig. 2 Historical and projected wind turbine costs. (**a**) shows the offshore wind turbine bid prices of existing projects. "Without" indicates that the tower is excluded, "With" indicates that the tower is included, "Unknown" means the inclusion of the tower is unclear. (Original data is in Supplementary Table 1) (**b**) shows the projection of wind turbine cost excluding the tower based on the learning curve.

Step3: Gridded assessment of offshore wind technology costs. *Development and marine use cost.* Development costs encompass expenses related to environmental, meteorological, and seabed surveys, project management, and development services, and are set at a fixed value of $230/kW[24]. The marine use cost is fixed at $94/kW[38].

Wind turbine cost. Based on tender cost data from early 2019 to July 2024, bid prices for turbines decreased from $700-$1200/kW before 2020 to $400-$700/kW after 2022, driven by economies of scale and the phaseout of subsidies (Fig. 2(a)). By 2023, the average bid price, excluding the tower, dropped to $420 per kW, reflecting a significant reduction of 45% compared to the 2019–2020 period. Assuming a one-year lag between the bidding and construction periods, we project the average turbine cost using a one-factor learning curve between the cumulative installed capacity and turbine cost. The learning rate is estimated at 25%, with a 90% confidence interval ranging from 12% to 36%. Consequently, the projected turbine cost is expected to fall to $242 (with a range of $180-$325) per kW by 2035 (Fig. 2(b)).

Tower cost. The tower cost decreases slightly with the growth of rated power. The tower cost per kW C_{tower} is the product of tower weight per kW W_{cap}, and the unit price A_{tower}. W_{cap} is negatively correlated with the rated power, as depicted in Eqs. (3, 4).

$$C_{tower} = A_{tower} W_{cap} \tag{3}$$

$$W_{cap} = -a_{tower} \ln(P) + b_{tower} \tag{4}$$

where A_{tower} equals to 1.25$/kg, a_{tower} is 12.63 kg/kW, b_{tower} is 89.5 kg/kW.

Foundation cost. Monopile and jacket foundations are two types of fixed foundations, used in water depths of up to 60 and 80 m, respectively. The amount of steel required for fixed foundations increases with water depth. Compared to monopile, jacket foundations, which feature multiple legs, are less sensitive to changes in rated power and water depth. As rated power and water depth increase, jacket foundations become more economically viable than monopile. The investment cost per unit capacity for fixed foundations, denoted as C_x (in $/kW) is related to the foundation weight per turbine W_x (in tons), price of unit weight A_x(in $/t), and the rate power P (in MW), as shown in Eq. (5). The foundation weight is influenced by water depth (in m) and P, as described in Eq. (6).

	A_x	a_x	b_x	c_x	d_x
	$/t	t	t/m	t/MW	t/(MW·m)
Monopile	1.23	70.15	3.20	93.39	3.04
Jacket	1.34	1514	16.3	28.9	0.18

Table 3. Function parameters of costs for monopile and jacket foundation.

Material	Price	WindFloat	Spar-Buoy	Hexofloat
Steel	1400$/t	3355t	2323t	2350t
Iron powder	140$/t			2000t
Concrete	70$/m3		2671m3	
Rated Power of Case		5 MW	5 MW	10 MW
Estimated Flatform Cost		939$/MW	688$/MW	357$/MW

Table 4. Material mass and cost estimates for three offshore wind floating platforms.

$$C_x = A_x W_x/(1000\mathrm{P}) \tag{5}$$

$$W_x = a_x + b_x\mathrm{depth} + c_x\mathrm{P} + d_x\mathrm{depth}\cdot\mathrm{P} \tag{6}$$

where parameters a_x, b_x, c_x are calibrated based on theoretical analysis[39] and engineering data (Supplementary Table 2). Values are summarized in Table 3.

China currently has only three floating offshore wind demonstration projects, all of which are based on steel semi-submersible platforms that use mooring and anchors to secure the platforms to the seabed. The platform cost of demonstration projects is $1320 per MW, but is expected to decline under technical change. We assume that by 2035, the floating structures and mass will correspond to the WindFloat, Spar-Buoy, and Hexofloat platforms under low, medium, and high scenarios, respectively[40]. Table 4 summarizes the mass and price of three materials, and estimates the cost of three platforms. We then apply a mass-based scaling law to adjust the platforms' mass accounting for the growth of rated power for 2035[36]. The costs are assumed to decline exponentially from 2022 to 2035.

Mooring & anchor cost. The cost of mooring lines is influenced by the number, length, density, unit cost of the lines, and the mass per unit rated power, with the length positively correlated with water depth, as shown in Eq. (7). The cost of anchors is determined by the number of mooring lines and the unit anchor cost, as outlined in Eq. (8). For a demonstrated floating offshore wind turbine in China with the rated power of 6.2 MW, nine mooring lines, each about 1000 m long are used, resulting in a cost of up to $1200 per kW. Mooring and anchor costs can be reduced by minimizing the number of mooring lines, optimizing their length, leveraging economies of scale, and using alternative materials. The parameters for these costs under three technical change scenarios are set based on previous research and engineering data[24,40]. Table 5 summarized the parameters and their values in three scenarios by 2035.

The costs are assumed to decline exponentially from 2022 to 2035.

$$PC_{mooring} = n_{lines}\left[(\alpha \times depth + \beta)\rho_{line}C_{line}\right]/P_0 \times W_t/W_0 \tag{7}$$

$$PC_{anchor} = n_{lines}C_{anchor}/P_0 \times W_t/W_0 \tag{8}$$

where $PC_{mooring}$ is the mooring cost per unit rated power (in $/kW), and PC_{anchor} is the anchor cost per unit rated power (in $/kW).

Transmission cost. The study considers two types of transmission technologies: High Voltage Alternating Current (HVAC) and High Voltage Direct Current (HVDC). HVAC systems have higher variable cable costs and lower fixed costs for substations, while HVDC systems feature lower cable costs but higher fixed costs for converter stations. Transmission costs (including installation) are modeled as a linear function of offshore distance, as shown in Eq. 9. The fixed costs (δ) for HVAC and HVDC are set at $166/kW and $470/kW, respectively, while the variable costs (γ) are $5.2/(kW·km) for HVAC and $2.2/(kW·km) for HVDC[41]. The U.S. Department of Energy has proposed a 35% cost reduction for HVDC by 2035. Since HVAC technology is more mature than HVDC, it is assumed that HVAC costs will decrease by 20%, 10%, and 0% under high, medium, and low scenarios, respectively. In contrast, HVDC costs are projected to decrease by 35%, 20%, and 5% under three scenarios. These cost reductions are assumed to occur linearly from 2022 to 2025.

$$C_{trans} = \gamma \times Dist + \delta \tag{9}$$

Parameter	Notation	Unit	Medium	High	Low
Number of mooring lines[a]	n_{lines}		6	3	9
Scale factor of variable length of mooring lines[b]	α	1	1.5	1.5	1.5
Fixed length of mooring lines[b]	β	m	460	680	900
Density of mooring line	ρ_{line}	t/m	0.18		
Unit cost of mooring line	C_{line}	$/t	210		
Cost of one anchor	C_{anchor}	k$	210		
Rated power of case	P_0	MW	6.25		
Averaged turbine and tower mass of case	W_0	t/MW	112.5		
Averaged turbine and tower mass in 2035 based on mass-based scaling law	W_t	t/MW	102.3	100.5	104.2

Table 5. Parameters for mooring and anchor costs under three scenarios for 2035. Note: [a]WindFloat and Spar-Bouy each use three mooring lines, Hexofloat uses six lines, and China's case turbine uses nine mooring lines. [b]According to Martinez and Iglesias[24], α is set at 1.5, β is derived as 460 m. β of China's case turbine is derived as 900 m.

Category	Name	Unit/Value
Dynamics	Time	Year
Geographic features	Longitude	°E
	Latitude	°N
	Province	10 Provinces
	Water depth	m
	Offshore distance	km
Turbine characteristics	Rated power	MW
	Rotor diameter	m
	Hub height	m
	Nacelle weight	t/MW
Technology selection	Foundation type	Monopile, Jacket, Floating
	Transmission type	HVAC, HVDC
Technology costs	Development cost	$/kW
	Marine use cost	$/kW
	Turbine cost	$/kW
	Tower cost	$/kW
	Foundation cost	$/kW
	Mooring & anchor cost	$/kW
	Transmission cost	$/kW
	Installation cost	$/kW
	Annual O&M cost	$/kW
Resource	Capacity factor	%
Power generation costs	LCOE	$/MWh
	CAPEX	$/MWh
	OPEX	$/MWh

Table 6. Description of variables in Data_*.nc files.

where C_{trans} is the transmission cost (in $/kW), *Dist* is the offshore distance (in km), γ is variable cost (in $/(kW·km)), and δ is fixed cost (in $/kW).

Installation cost. Due to differences in installation approaches and locations, the installation costs for monopile, jacket-type and floating wind turbines vary, with estimates of $1.79 million, $2.15 million, and $0.77 million per turbine, respectively[28]. Floating projects also incur additional installation costs for the mooring system, set at $270000 per turbine[24]. The unit installation costs are $179, $215 and $104/kW for a 10 MW turbine, respectively. For fixed foundations, installation costs are assumed to reduce with the growth in rated power. For floating wind projects in China, the current installation cost exceeds $900/kW, and it is projected to decrease to $100, $200, and $300/kW under high, medium, and low scenarios[42], respectively, with annual exponential reductions from 2022 to 2030.

O&M cost. Operation and Maintenance (O&M) costs are primarily influenced by turbine type and offshore distance. The annual fixed O&M costs for fixed and floating offshore wind farms are set as $19.7 and $20.8/kW, respectively, with variable O&M costs per distance at $0.013 and $0.022/(kW·km)[29]. Based on actual engineering

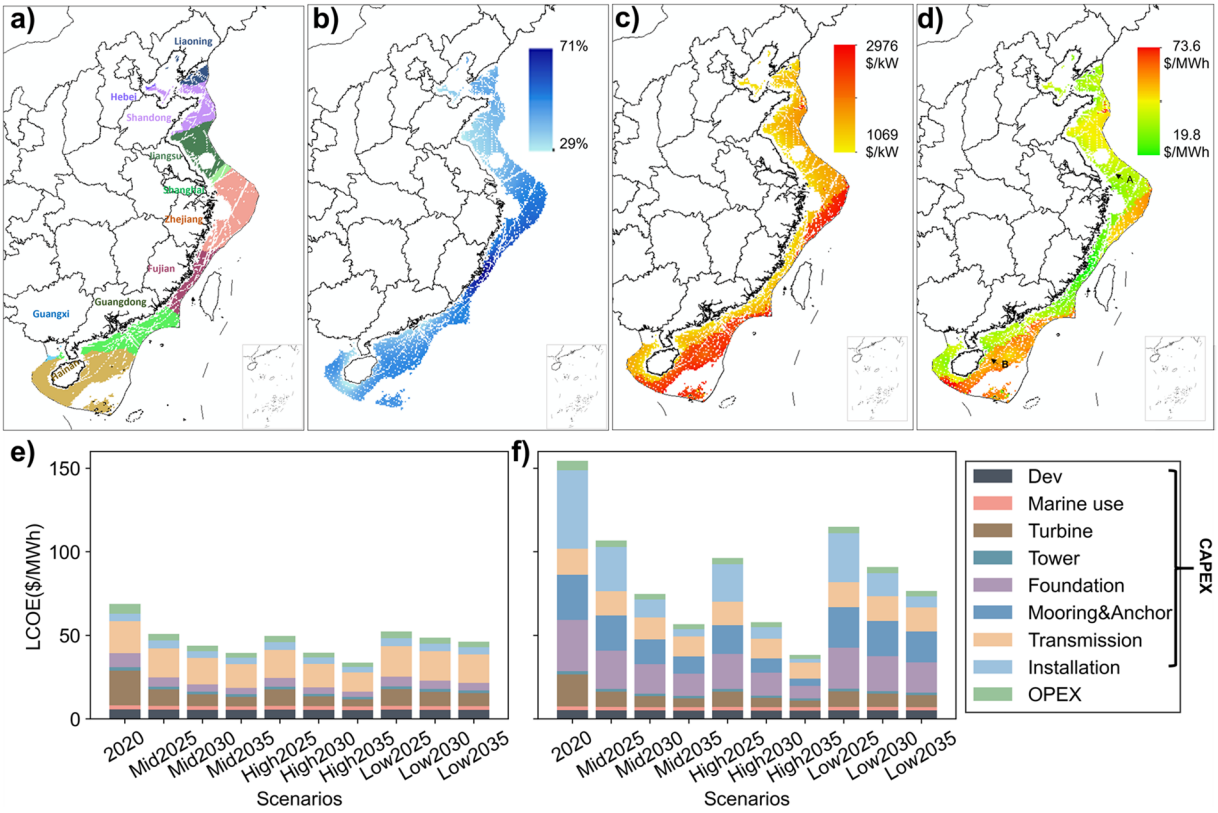

Fig. 3 Offshore wind resource and costs in China. (**a**) displays the provinces closest to available offshore wind sites; (**b**–**d**) show the capacity factors, investment costs and LCOE in 2035 under the medium scenario; (**e**) presents the LCOE breakdown for fixed offshore wind at point A in (**d**), and (**f**) shows the LCOE breakdown for floating offshore wind at point B in (**d**).

data from China, the annual O&M costs for 3 MW and 6 MW fixed turbines are $29.6 and $19.7/kW, respectively. This indicates that for every 1% increase in capacity, O&M costs decrease by 0.33%. This relationship allows for modeling the changes in O&M costs under three scenarios.

Step4: Assessment of offshore wind LCOE. LCOE represents the ratio of all discounted costs incurred over the lifetime of an energy project to the total electricity produced, as shown in Eq. (10). It is commonly used to assess the economic feasibility of power generation projects. We also analyze the components of LCOE, including all capital and operational expenses, as outlined in Eqs. (11, 12). Based on the gridded LCOE estimates, we map the cost curve for all coastal regions and compare it to the baseline cost of coal-fired power to assess the economic potential of offshore wind.

$$LCOE = \frac{\sum_{i=1}^{I} CAP_i + \sum_{t=1}^{T} OM_t (1+r)^{-t}}{\sum_{t=1}^{T} 8760 CF_t (1+r)^{-t}} \tag{10}$$

$$CAPEX_i = \frac{CAP_i}{\sum_{t=1}^{T} 8760 CF_t (1+r)^{-t}} \tag{11}$$

$$OPEX = \frac{\sum_{t=1}^{T} OM_t (1+r)^{-t}}{\sum_{t=1}^{T} 8760 CF_t (1+r)^{-t}} \tag{12}$$

where CF_t is the capacity factor of year t, assumed to be the value of the installation year; CAP_i represents all types of investment costs; OM_t denotes the O&M costs for each year; r is discounted rate, set as 8%; and T is the lifetime of the offshore wind project, assumed to be 25 years. $CAPEX_i$ refers to the levelized investment cost of each component, and OPEX is the levelized O&M cost.

Nomenclatures	Units	Details
CapacityFactor _*.tif	%	Capacity factors of offshore wind in each grid, including 6 maps (2020, 2025, 2030, and 2035 of medium scenario, and 2035 of high and low scenarios); considering the change of hub height under different scenarios
InvestmentCost _*.tif	$/kW	Investment costs of offshore wind in each grid, including 6 maps (same as capacity factor maps)
LCOE_*.tif	$/MWh	LCOE of offshore in each grid, including 6 maps (same as capacity factor maps)
Data_*.nc		25 variables related to offshore wind in 5058 grid points and 16 years (2020–2035) (Details in Supplementary Table 6),
Wind_hourly_outputs_2020.nc	%	8760 h capacity factors of offshore wind in each grid point and in year 2020

Table 7. Nomenclature of data files and detailed explanations.

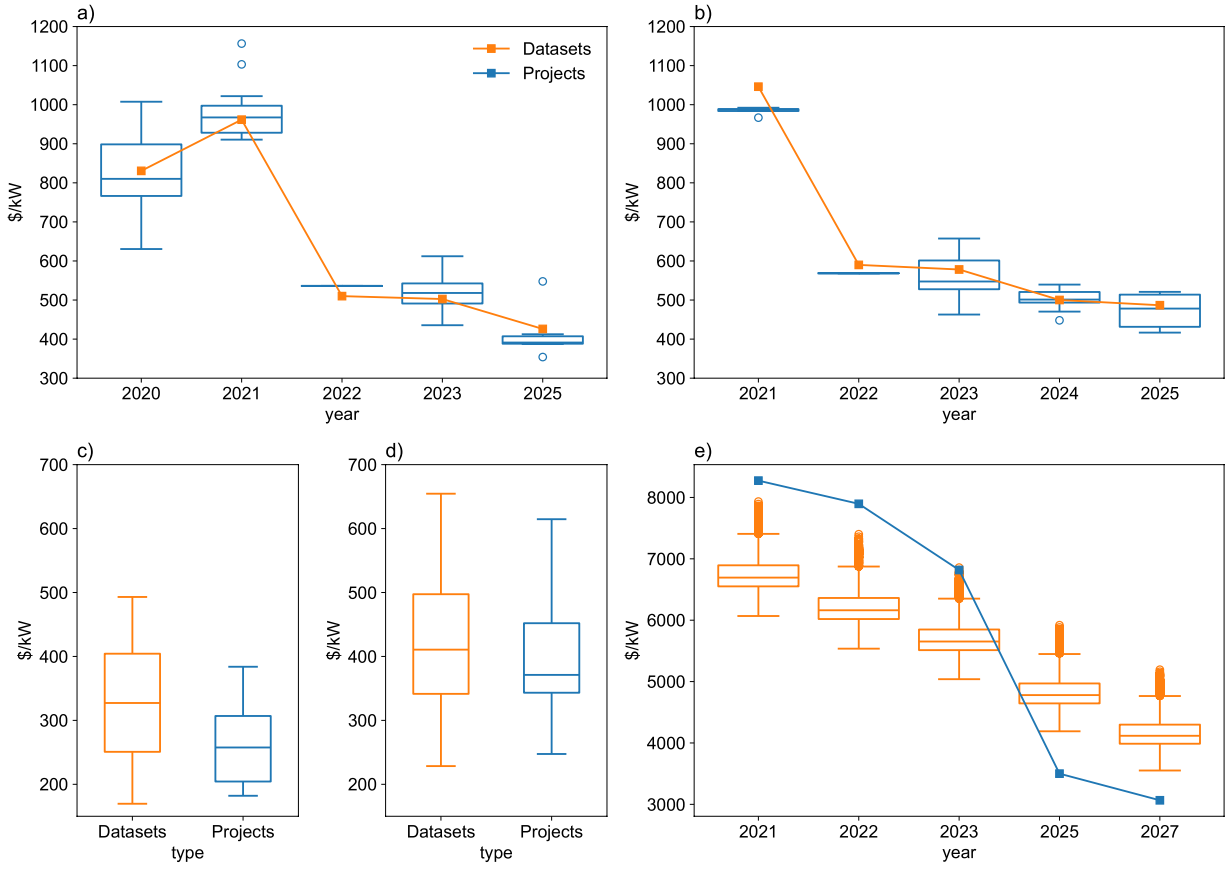

Fig. 4 Comparison of investment costs between datasets and actual project data. (**a**) shows offshore wind turbine costs (exclude tower), assuming a one-year lag between the bidding and construction period; (**b**) shows offshore wind turbine costs (include tower), assuming a one-year lag; (**c**) depicts monopile foundation costs; (**d**) depicts jacket foundation costs in 2020; (**e**) is about total investment costs of floating offshore wind.

Data Records

We provide three datasets for users. The first dataset contains 25 features of offshore wind at 5058 grid points with a 10 km resolution, under three technical change scenarios from 2020 to 2035, and stored in three NetCDF(.nc) files. The features include one temporal variable, five geographic features, four turbine characteristics, two technology selection variables (foundation and transmission), nine technology costs by components, one resource variable, and three generation cost variables (Table 6). Fig. 3(a) shows the spatial distribution of available offshore wind power, while Fig. 3(e,f) presents the generation costs and their components for fixed and floating wind power at two locations. The second dataset includes spatial distribution maps of capacity factors, investment costs, and LCOE for typical years (2020, 2025, 2030, and 2035 in the medium scenario, and 2035 in the high and low scenarios), stored in 18 GeoTIFF files at a 10 km resolution. Fig. 3(b–d) depict the spatial distribution of these three variables for 2035 in the medium scenario. The third dataset offers hourly output curves for offshore wind power over 8760 hours at the 5058 grid points in 2020, stored in a NetCDF file. These datasets offer a comprehensive resource for global, national, and sub-regional offshore wind power research and policy analysis, and are available via figshare[43]. Table 7 provides details of the nomenclatures and additional information about the datasets.

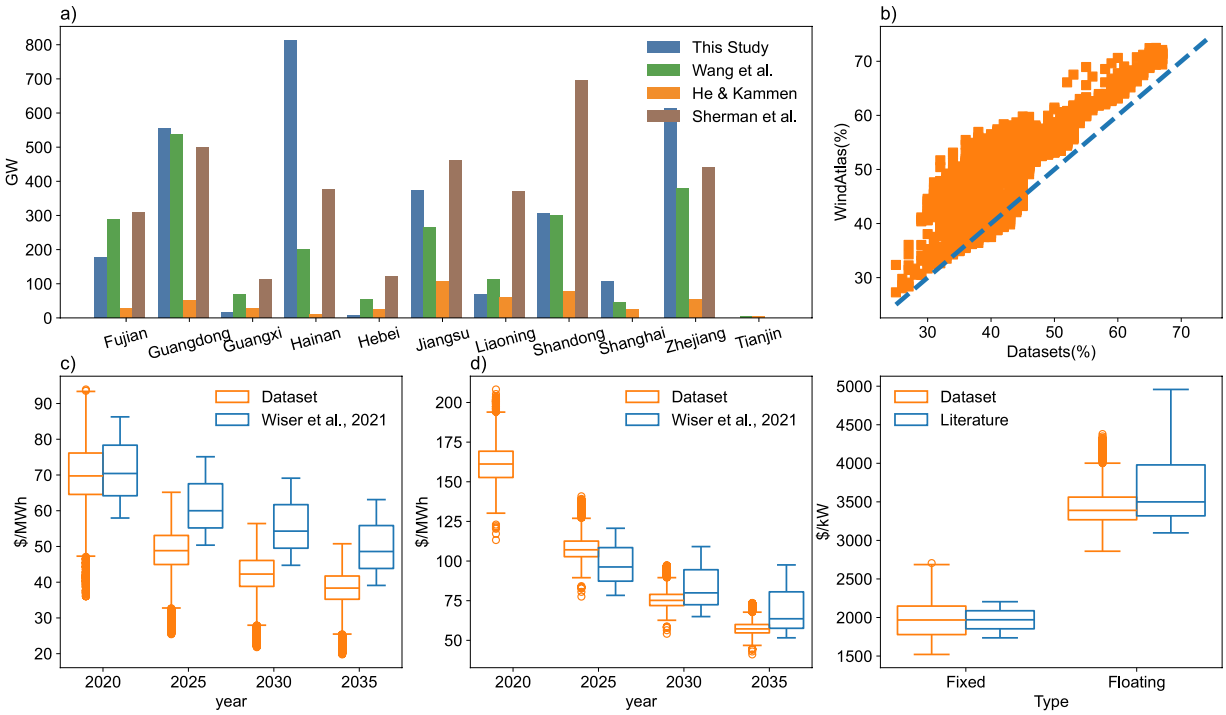

Fig. 5 The comparison of capacity potential, capacity factors and technical change scenarios with existing datasets. (**a**) shows the comparison of offshore wind capacity potential[32,44,45]; (**b**) depicts the comparison of offshore wind capacity factors between this dataset and Global Wind Atlas[18]; (**c**) is LCOE of fixed-bottom offshore wind, and (**d**) is LCOE of floating offshore wind compared to the median scenario of Wiser *et al.*[33]; (**e**) is the comparison of fixed-bottom offshore wind investment costs between year 2023 of this dataset and existing studies[34,38], and the comparison of floating offshore wind investment costs between year 2030 of this dataset and existing studies[25,26,34].

Technical Validation

Comparison with actual projects. China has numerous fixed-bottom offshore wind projects and a few floating offshore wind projects. This study compares the costs in the dataset with those of actual projects to verify the accuracy and consistency. First, we compared the wind turbine costs from the dataset with the bidding costs of 116 fixed offshore wind projects awarded between 2019 and 2024. The dataset's estimated costs align with actual project data (Fig. 4(a,b)). Second, we compared the monopile and jacket foundation costs from the dataset with those of actual projects. Although the average cost is slightly higher, due to a greater average water depth for monopile and jacket foundations in the dataset compared to actual projects, the cost range in the dataset encompasses the costs of existing projects, indicating consistency in foundation costs (Fig. 4(c,d)). Finally, we compared the total investment costs of floating offshore wind projects in the dataset with the costs of five commissioned or planned projects. The analysis reflects dynamic cost changes from 2021 to 2027, with the costs of projects in 2025 and 2027 falling within the medium to high ranges of technical change, further validating both the investment costs and technical change assumptions (Fig. 4(e)).

Comparison with existing datasets and literatures. We also compared this dataset with existing datasets and literatures related to installed capacity potential, capacity factors, and technology costs to identify similarities and differences, thereby validating the accuracy of this dataset.

First, the potential assessed in this dataset is 3035 GW, which falls within the range of existing studies (Fig. 5(a)). Wang *et al.*[44] estimated the capacity potential as 2253 GW considering areas where the offshore distance is between 10 km and 200 km, and the water depth is less than 100 m. However, this approach ignores areas with deeper waters and farther offshore distances, and does not account for space availability constraints. This leads to higher estimates for Fujian, Hebei, and Liaoning, due to the exclusion of constraint conditions, while estimates for Hainan and Zhejiang are lower because deep-water and far-offshore areas are omitted. He and Kammen[45] evaluated a potential of 469 GW but their analysis is limited to areas with waters of less than 20 m, therefore, which is far less than the estimation of this dataset. Sherman *et al.*[32] reported the potential as 3389 GW, which is slightly higher than our estimates but differs significantly at the provincial level. The discrepancy is mainly because Sherman *et al.* only considers areas with water depths of less than 60 m and did not incorporate constraint conditions. Second, the capacity factors assessed in this dataset are largely consistent with existing datasets, with a correlation coefficient of 0.83 (Fig. 5(b)). However, the capacity factors for each grid in this study are generally lower than those reported in previous research[33], with an average of 43% compared to 50%. This difference can be attributed to the application of a bias correction method that adjusts wind speed data downward, better consistent with actual project conditions.

Regarding technology costs, when comparing the medium technical change scenarios from this study and Wiser *et al.*[33], the LCOE estimates for fixed-bottom offshore wind in 2020 are largely consistent (Fig. 5(c)). However, the LCOE projections for 2025 in this study are significantly lower than the results of Wiser *et al.*, primarily due to the sharp decline in offshore wind turbine costs in China over the past three years. The forecasts for the reduction in fixed-bottom offshore wind costs from 2025 to 2035 are generally consistent between both studies. For floating offshore wind, the LCOE projections for 2025, 2030, and 2035 in this study are closely aligned with Wiser *et al.* (Fig. 5(d)). We also compare the investment costs for both fixed-bottom and floating offshore wind between this dataset and existing studies[25,26,34,38] (Fig. 5(e)). The results show strong alignment with previous estimates, further confirming the robustness and accuracy of this dataset.

Usage Notes

The dataset offers gridded offshore wind power capacity potential, costs, hourly output curves for each grid, and their dynamic evolution under three technical change scenarios. Users can aggregate and process this data as needed, serving as foundational inputs for integrated assessment models, energy system models, power system models, and marine energy technology modeling. For integrated assessment and energy system models with annual resolution and regional scale, users can generate cost curves—specifically, the relationships between LCOE and cumulative electricity generations—and incorporate these cost curves in a linearized form into the models. For power system optimization models with hourly resolution and regional scale, users can cluster typical hourly output curves at the regional scale, and integrate them into the model for optimizing economic dispatch. Some power system models are developed at the grid scale with hourly resolution to capture spatial complementarity and optimize the spatial layout of renewable energy technologies[9,46]. This dataset fully meets the data requirements of such models. In marine energy technology modeling, this dataset can be used to quantify the potential for synergistic deployment of various marine energy sources, such as evaluating the role of co-located offshore wind and solar power in improving marine utilization efficiency and reducing transmission costs and OPEX. The impact of climate change, ecological protection, and marine planning on the cost-effectiveness of offshore wind power can be assessed using this dataset as the base data. This dataset excludes most existing offshore wind farms due to the constraints related to minimum offshore distance and water depth, and users can supplement it with other open-source[37] or commercial datasets. Uncertainties related to technical change can be dynamically updated annually through ongoing interaction with engineering experts.

Code availability

The code used for generating China's offshore wind potential and costs dataset is written in Python and available from https://github.com/KennethAnn/OffshoreWindDataset. The VWF model is available from https://github.com/renewables-ninja/vwf.

Received: 3 November 2024; Accepted: 3 January 2025;
Published online: 14 January 2025

References

1. Li, L. *et al*. Mitigation of China's carbon neutrality to global warming. *Nat Commun* **13**, 5315 (2022).
2. Davis, S. J. *et al*. Net-zero emissions energy systems. *Science* **360**, (2018).
3. Duan, H. *et al*. Assessing China's efforts to pursue the 1.5°C warming limit. *Science* **372**, 378–385 (2021).
4. Bogdanov, D. *et al*. Radical transformation pathway towards sustainable electricity via evolutionary steps. *Nat Commun* **10**, 1077 (2019).
5. An, K., Wang, C. & Cai, W. Low-carbon technology diffusion and economic growth of China: an evolutionary general equilibrium framework. *Structural Change and Economic Dynamics* **65**, 253–263 (2023).
6. He, G. *et al*. Rapid cost decrease of renewables and storage accelerates the decarbonization of China's power system. *Nat Commun* **11**, 2486 (2020).
7. Wang, Y. *et al*. Accelerating the energy transition towards photovoltaic and wind in China. *Nature* **619**, 761–767 (2023).
8. Lu, X. *et al*. Challenges faced by China compared with the US in developing wind power. *Nat Energy* **1**, 1–6 (2016).
9. Zhang, D. *et al*. Spatially resolved land and grid model of carbon neutrality in China. *Proc. Natl. Acad. Sci. U.S.A.* **121**, e2306517121 (2024).
10. O'Shaughnessy, E. *et al*. Community solar reaches adopters underserved by rooftop solar. *Nat Energy* **9**, 926–927 (2024).
11. Guo, X. *et al*. Grid integration feasibility and investment planning of offshore wind power under carbon-neutral transition in China. *Nat Commun* **14**, 2447 (2023).
12. Global Wind Energy Council. Global Offshore Wind report 2024. https://gwec.net/global-offshore-wind-report-2024 (2024).
13. Millstein, D. *et al*. A database of hourly wind speed and modeled generation for US wind plants based on three meteorological models. *Sci Data* **10**, 883 (2023).
14. Jensen, T. V. & Pinson, P. RE-Europe, a large-scale dataset for modeling a highly renewable European electricity system. *Sci Data* **4**, 170175 (2017).
15. Zheng, C. Temporal-spatial characteristics dataset of offshore wind energy resource for the 21st Century Maritime Silk Road. *CSD* **5**, 21.86101.1/csdata.2020.0097.zh (2020).
16. Zheng, C. & Pan, J. Assessment of the global ocean wind energy resource. *Renewable and Sustainable Energy Reviews* **33**, 382–391 (2014).
17. Zheng, C. *et al*. Assessing the China Sea wind energy and wave energy resources from 1988 to 2009. *Ocean Engineering* **65**, 39–48 (2013).
18. Davis, N. *et al*. The Global Wind Atlas: A high-resolution dataset of climatologies and associated web-based application. *Bulletin of the American Meteorological Society* **104**, E1507–E1525 (2023).
19. Lu, X. *et al*. Global potential for wind-generated electricity. *Proceedings of the National Academy of Sciences* **106**, 10933–10938 (2009).
20. Staffell, I. & Pfenninger, S. Using bias-corrected reanalysis to simulate current and future wind power output. *Energy* **114**, 1224–1239 (2016).
21. Jiang, H. *et al*. Assessment of offshore wind-solar energy potentials and spatial layout optimization in mainland China. *Ocean Engineering* **287**, 115914 (2023).

22. Hong, L. & Möller, B. Offshore wind energy potential in China: Under technical, spatial and economic constraints. *Energy* **36**, 4482–4491 (2011).
23. Möller, B. Continuous spatial modelling to analyse planning and economic consequences of offshore wind energy. *Energy Policy* **39**, 511–517 (2011).
24. Martinez, A. & Iglesias, G. Multi-parameter analysis and mapping of the levelised cost of energy from floating offshore wind in the Mediterranean Sea. *Energy Conversion and Management* **243**, 114416 (2021).
25. Maienza, C. *et al*. A life cycle cost model for floating offshore wind farms. *Applied Energy* **266**, 114716 (2020).
26. Díaz, H. & Guedes Soares, C. Cost and financial evaluation model for the design of floating offshore wind farms. *Ocean Engineering* **287**, 115841 (2023).
27. Judge, F. *et al*. A lifecycle financial analysis model for offshore wind farms. *Renewable and Sustainable Energy Reviews* **103**, 370–383 (2019).
28. Myhr, A. *et al*. Levelised cost of energy for offshore floating wind turbines in a life cycle perspective. *Renewable Energy* **66**, 714–728 (2014).
29. Bosch, J. *et al*. Global levelised cost of electricity from offshore wind. *Energy* **189**, 116357 (2019).
30. Castro-Santos, L. *et al*. Economic Feasibility of Floating Offshore Wind Farms in the North of Spain. *Journal of Marine Science and Engineering* **8**, 58 (2020).
31. Castro-Santos, L. *et al*. Economic feasibility of floating offshore wind farms in Portugal. *Ocean Engineering* **207**, 107393 (2020).
32. Sherman, P. *et al*. Offshore wind: An opportunity for cost-competitive decarbonization of China's energy economy. *Science Advances* **6**, eaax9571 (2020).
33. Wiser, R. *et al*. Expert elicitation survey predicts 37% to 49% declines in wind energy costs by 2050. *Nature Energy* **6**, 555–565 (2021).
34. Santhakumar, S. *et al*. Technological learning potential of offshore wind technology and underlying cost drivers. *Sustainable Energy Technologies and Assessments* **60**, 103545 (2023).
35. Molod, A. *et al*. Development of the GEOS-5 atmospheric general circulation model: evolution from MERRA to MERRA2. *Geosci. Model Dev.* **8**, 1339–1356 (2015).
36. Sergiienko, N. Y. *et al*. Review of scaling laws applied to floating offshore wind turbines. *Renewable and Sustainable Energy Reviews* **162**, 112477 (2022).
37. Zhang, T. *et al*. Global offshore wind turbine dataset. *Sci Data* **8**, 191 (2021).
38. Du, J. *et al*. Construction Cost Trend Analysis of Offshore Wind Power and Investment Suggestions of Petrochemical Industry. *Engineering Cost Management* 85–91 (2022).
39. Tang W. *et al*. Techno-economic Analysis of Key Equipment for Offshore Wind Farms with Multiple Scenarios. *Electric Power* **54**, 07 (2020).
40. Ghigo, A. *et al*. Platform Optimization and Cost Analysis in a Floating Offshore Wind Farm. *Journal of Marine Science and Engineering* **8**, 835 (2020).
41. Wu Q. *et al*. Techno-Economic Analysis of Far Coast Offshore Wind Power Transmission Modes. *Electrotechnics Electric* 1–9+15 (2024).
42. Liu, G. *et al*. Study on cost comparison and variation trend of floating offshore wind power between China and Europe. *Express Water Resources & Hydropower Information* **45**, 70–73+80 (2024).
43. An, K., Cai, W., Lu, X. & Wang, C. High-resolution gridded dataset of China's offshore wind potential and costs under technical change. *Figshare* https://doi.org/10.6084/m9.figshare.27230862.
44. Wang, Y., Chao, Q., Zhao, L. & Chang, R. Assessment of wind and photovoltaic power potential in China. *Carb Neutrality* **1**, 15 (2022).
45. He, G. & Kammen, D. M. Where, when and how much wind is available? A provincial-scale wind resource assessment for China. *Energy Policy* **74**, 116–122 (2014).
46. Beiter, P., Mai, T., Mowers, M. & Bistline, J. Expanded modelling scenarios to understand the role of offshore wind in decarbonizing the United States. *Nat Energy* **8**, 1240–1249 (2023).
47. Flanders Marine Institute. Maritime Boundaries Geodatabase: Maritime Boundaries and Exclusive Economic Zones (200NM), version 12. https://doi.org/10.14284/632 (2023).
48. NOAA National Centers for Environmental Information. ETOPO 2022 15 Arc-Second Global Relief Model. https://doi.org/10.25921/fd45-gt74 (2022).
49. Bohorquez, J. *et al*. China's little-known efforts to protect its marine ecosystems safeguard some habitats but omit others. *Science Advances* **7**, eabj1569 (2021).
50. Yong, D. L. *et al*. Migratory songbirds in the East Asian-Australasian Flyway: a review from a conservation perspective. *Bird Conservation International* **25**, 1–37 (2015).
51. Benden, P. Global Shipping Lanes (1.4). https://doi.org/10.5281/zenodo.6361813 (2022).
52. Wang, J. & Zuo, W. China's coastal routes, inland routes and ports. *Geographical Atlas of China*. https://www.osgeo.cn/map/m0183 (2010).
53. TeleGeography. Submarine Cable Map. https://www.submarinecablemap.com (2024).
54. Global Energy Monitor. Global Oil and Gas Extraction Tracker. https://globalenergymonitor.org/projects/global-oil-gas-extraction-tracker/ (2024).
55. Halpern, B. S. *et al*. Spatial and temporal changes in cumulative human impacts on the world's ocean. *Nat Commun* **6**, 7615 (2015).
56. Enclive. Electronic Navigational Charts. http://map.enclive.cn (2024).

Acknowledgements

This work is jointly supported by National Natural Science Foundation of China (No. 72348001 and No. T2261129475).

Author contributions

K.A. and C.W. designed and conceptualized the study and generated the dataset. K.A. and W.C. conducted the analysis and wrote the manuscript. K.A. and X.L. revised the manuscript. C.W. directed the research group.

Competing interests

The authors declare no competing interests.

Additional information

Supplementary information The online version contains supplementary material available at https://doi.org/10.1038/s41597-025-04428-8.

Correspondence and requests for materials should be addressed to C.W.